Journal of Materials Chemistry

Cite this: *J. Mater. Chem.*, 2011, **21**, 15057

www.rsc.org/materials

PAPER

Templating synthesis of uniform Bi_2Te_3 nanowires with high aspect ratio in triethylene glycol (TEG) and their thermoelectric performance†

Kai Wang, Hai-Wei Liang, Wei-Tang Yao and Shu-Hong Yu*

Received 27th May 2011, Accepted 20th July 2011
DOI: 10.1039/c1jm12384j

Highly uniform Bi_2Te_3 nanowires with a length of tens of micrometres and a diameter of 15–17 nm can be synthesized through a simple and fast solution process by using ultrathin Te nanowires as sacrificial templates. Different from previous template-directed hydrothermal synthesis, here we used heating mantle as the reactor for preparing Bi_2Te_3 nanowires, which not only makes the reaction perform more efficiently and be finished within one hour, but also can achieve more uniform nanowires. As-synthesized Bi_2Te_3 nanowires have a hexagonal-phase single crystalline structure. It was found that using triethylene glycol (TEG) as solvent and precise controlling reaction temperature and time were crucial to obtain high-quality single crystal Bi_2Te_3 nanowires. The formation process of Bi_2Te_3 nanowires was believed to include both Kirkendall effect and Ostwald ripening, according to the experimental observations. Compared with other Bi_2Te_3 nanostructures and bulk Bi_2Te_3 materials, the thermal conductivity of Bi_2Te_3 nanowire pellet decreased evidently, verifying that one-dimensional thermoelectric nanomaterials indeed exhibit lower thermal conductivity.

Introduction

During the past few decades, with the rapid development of human society, the consumption of traditional energy has increased exponentially. Therefore, more and more researchers come to pay close attention to new energy sources. Thermoelectric (TE) device emerges as a new kind of hot material that can directly achieve the conversion between heat and electricity, which can maximize the use of waste heat and electricity in daily life. The efficiency of the thermoelectric device is related to the figure of merit $ZT = (S^2\sigma/\kappa)T$, where S is the Seebeck coefficient, σ is the electrical conductivity, κ is the thermal conductivity, and T is the absolute temperature.[1] The higher the ZT is, the higher the conversion efficiency.

Bi_2Te_3, as a hot TE material that can show a high ZT around the room temperature, has been acknowledged and researched extensively.[2] Recently, a bulk p-type Bi_2Te_3 which was synthesized through a ball-milling process followed directly hot pressing with the highest value $ZT \approx 1.4$ have been reported by Poudel *et al.*[3] Whereas, the numerical value related to the efficiency was not high enough for large-scale production and utilization. After much of research on the thermoelectric materials, Dresselhaus *et al.* proposed that the figure of merit ZT of TE materials in one-dimensional (1D) nanostructures could be improved noticeably by reducing the thermal conductivity,[4,5] which has been testified by both experimental studies and theoretical calculations.[3,6–14] So far, many Bi_2Te_3 nanostructures with various morphologies have been synthesized through different strategies, such as nanoparticle,[15,16] nanoplates,[17,18] nanocapsules[19] and hollow nanospheres.[20] And for synthesis of 1D Bi_2Te_3 nanostructures, the most commonly used methods were the traditional electrodeposition and template-directed electrodeposition methods.[21–25] Besides that, Bi_2Te_3 nanowires,[26,27] nanotubes,[28] and nanorods[29,30] have been prepared through hydrothermal and solvothermal routes. In addition, ordered Bi_2Te_3 nanowire arrays have also been fabricated *via* physical vapor deposition process.[31] Unfortunately, the Bi_2Te_3 nanowires synthesized by electrodeposition usually had relatively thicker diameter, while that were prepared by solution chemistry process were constantly inferior in quality.

Template-directed synthesis has been widely used for fabrication of 1D nanostructures during the past two decades.[32–34] Now, many 1D telluride nanostructures have been synthesized by using Te nanowire and nanorod as the template.[28,34,35] Recently, the ultrathin Te nanowires with a diameter of only several nanometres have been synthesized and used as an effective template to fabricated CdTe and PbTe nanowires by our group.[35,36] Different from the hydrothermal process for synthesis of CdTe and PbTe nanowires in our previous studies, herein we adopt the heating mantle as the reactor that was more facile and effective for synthesis of high-quality uniform Bi_2Te_3 nanowires. Because the heating mantle was connected to a digital temperature controller, it can heat up the solution at a preset heating rate.

Division of Nanomaterials and Chemistry, Hefei National Laboratory for Physical Sciences at Microscale, Department of Chemistry, Department of Materials of Science and Engineering, University of Science and Technology of China, Hefei, Anhui, 230026, P. R. China. E-mail: shyu@ustc.edu.cn; Fax: +86 551 3603040

† Electronic supplementary information (ESI) available: Fig. S1–S4 containing TEM, SEM, and XRD data. See DOI: 10.1039/c1jm12384j

The formation mechanism of the Bi_2Te_3 nanowires was also discussed. In addition, the thermoelectric transportation performance of the obtained Bi_2Te_3 nanowires has been investigated.

Experimental

Materials

All chemical reagents were analytical grade that can be commercially available from Shanghai Chemical Reagent Co. Ltd, and were used without further purification in this study.

Synthesis of ultrathin Te nanowires

The high-quality uniform ultrathin Te nanowires with a diameter of only several nanometres were prepared according to the previous method deveolped by our group.[36] In a typical synthesis, 1.000 g polyvinylpyrrolidone (PVP) and 0.092 g Na_2TeO_3 (0.42 mmol) were dissolved in 35 mL of double distilled water under vigorous magnetic stirring to form a homogeneous solution at room temperature. After that, 1.65 mL of hydrazine hydrate (85%, w/w%) and 3.35 mL of aqueous ammonia solution (25–28%, w/w%) were added into the mixed solution respectively. The final solution was transferred into a Teflon vessel with a total volume of 50 mL. Then, the container was closed and maintained at 180 °C for 3 h and cooled down to room temperature naturally. The product was precipitated by adding 110 mL of acetone into the Te nanowires solution.

Synthesis of Bi_2Te_3 nanowires

In a typical synthesis, 0.600 g polyvinylpyrrolidone (PVP) was first dissolved in 30 mL triethylene glycol (TEG) under vigorous magnetic stirring. After that, Te nanowires (~0.42 mmol) from the previous experiment were dispersed in the solution by stirring dramatically before 0.245 mmol $Bi(NO_3)_3 \cdot 5H_2O$ and 1 mL hydrazine hydrate were added as Bi source and reductant respectively. Finally, adequate NaOH was used to adjust the pH to 13. Then, the reaction was performed in a 50 ml three-neck flask equipped with a thermometer, glass tube and condenser. The mixture solution was then heated from room temperature to 200 °C at a rate of 10 °C per minute and kept at 200 °C for 20 min under magnetic stirring and nitrogen protection. After natural cooling to room temperature, the final product was centrifuged and washed several times with absolute alcohol and double distilled water, and then dried in vacuum at 60 °C.

Sample characterization

The obtained sample was characterized by an (Philips X'Pert Pro Super) X-ray powder diffractometer with Cu Ka radiation (λ = 1.541874 Å). Scanning electron microscopy (SEM) was performed with a field emission scanning electron microanalyzer (Zeiss Supra 40). Transmission electron microscopy (TEM) was performed on H-7650 (Hitachi, Japan) operated at an acceleration voltage of 100 kV. High-resolution transmission electron microscope (HRTEM) was operated on JEOL-2010 at an acceleration voltage of 200 kV. The energy dispersive X-ray spectroscopy (EDS) analysis was also done with a JEOL-2010 TEM with an Oxford windowless Si (Li) detector equipped with a 4-pulse processor.

Thermoelectric properties

To keep the nanowire structure of the sample, we just pressed the as-prepared powder into a pellet with dimensions of 10 mm × 4 mm × 1.5 mm at room temperature under a pressure of 40 MPa. The Seebeck coefficient and thermal conductivity were measured by a two-terminal method, while the electrical resistivity was measured *via* a four-probe resistance measurement. All figures were detected from 50 K to 300 K *via* using Physical Property Measurement System (PPMS) apparatus.

Results and discussion

The Te nanowires that were chosen as the template has a length of tens of micrometres and a diameter of only several nanometres (see ESI, Fig. S1†). Then the high quality Bi_2Te_3 nanowires were prepared *via* a facile solution phase method using the ultrathin Te nanowires as the template and triethylene glycol (TEG) as solvent. Fig. 1 shows the X-rays diffraction (XRD) pattern of the products obtained at 200 °C for 20 min in TEG. All the diffraction peaks are in good agreement with the standard literature of hexagonal-phase Bi_2Te_3 (JCPDS 72–2036). There were no other peaks in existence, indicating that the sample was pure Bi_2Te_3 crystalline phase without residual impurities. Scanning electron microscopy (SEM) and transmission electron microscopy (TEM) images in Fig. 2 confirmed the presence of abundant wire-like 1D nanostructures, and the nanowires have a length of tens of micrometres and a diameter of 15–17 nm. As the Bi atoms entered into the Te nanowires template, so the diameter of the Bi_2Te_3 nanowires was appreciably larger than that of Te template. To the best of our knowledge, such uniform and high-quality Bi_2Te_3 nanowires have never been synthesized by non-templating method.

The energy-dispersive X-ray spectroscopy (EDS) was detected on a random sample, testifying that the nanowires were composed of stoichiometric Bi_2Te_3 (Fig. 3). Additionally, a high resolution TEM (HRTEM) image taken from an individual nanowire shown in Fig. 4a, in which the lattice spacing was measured as 3.31 Å, corresponding to that for the (009) planes of the hexagonal Bi_2Te_3. It also can indicate that the nanowires

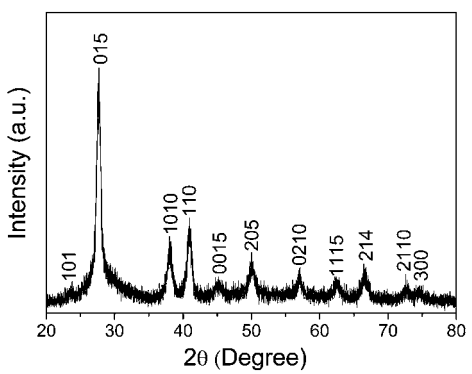

Fig. 1 XRD pattern of the obtained Bi_2Te_3 nanowires prepared in TEG at 200 °C for 20 min.

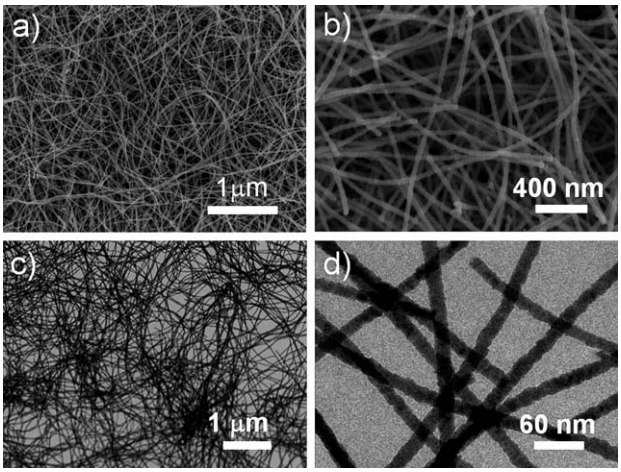

Fig. 2 Different magnifications of SEM images (a,b) and TEM images (c,d) of Bi_2Te_3 nanowires obtained in TEG at 200 °C for 20 min.

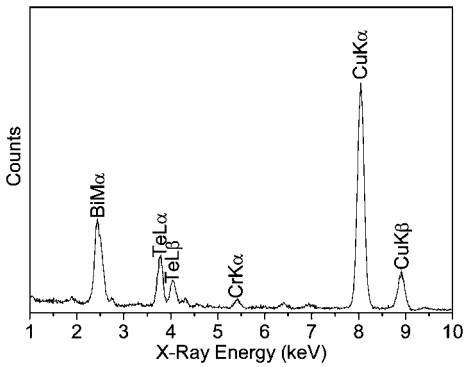

Fig. 3 EDS spectrum of the Bi_2Te_3 nanowires. The signals corresponding to Cu and Cr were contributed by the TEM grid.

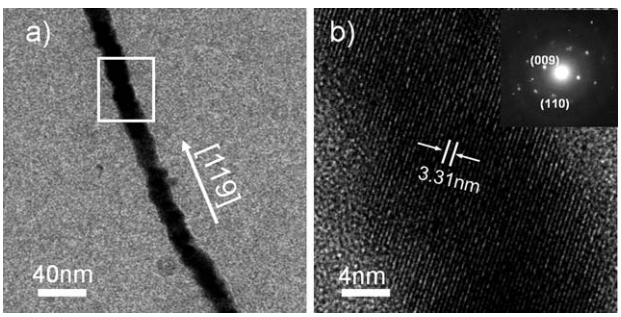

Fig. 4 (a) TEM image of an individual Bi_2Te_3 nanowire. (b) HRTEM image of the selected area of the Bi_2Te_3 nanowire shown in (a), the inset was the corresponding SAED pattern.

grow along the <119> direction. The corresponding selected area electron diffraction (SAED) pattern (the inset in Fig. 4b) could further confirm the above result. Both of the HRTEM image and the SAED pattern demonstrated the nanowires possessed a well single crystallinity. All the above results show that high-quality Bi_2Te_3 nanowires with uniform diameter and high aspect ratio have been prepared successfully through the template-assisted solution route and the Te nanowires with high active reaction are indeed perfect templates to synthesize 1D nanostructured materials.

The choice of template, reaction parameters, and reaction solvent played crucial roles for the synthesis of uniform Bi_2Te_3 nanowires that with high aspect radio and good quality. First, the ultrathin Te nanowires with a diameter of only several nanometres were chosen as templates due to their high reactivity and excellent dispensability in water, EG, TEG and other hydrophilic solvents, which can promote the formation of homogeneous nanostructured coating on the template.[35,36] Then, TEG also plays an important role in this template-reaction. The TEG as solvent has several obvious advantages, *i.e.*, (i) it is a nontoxic, pollution-free and environment-friendly solvent, and will not produce any by-product during the reaction process; (ii) it has a higher viscosity that can provide a stable reaction environment; (iii) its high boiling point can made the reaction carry out at a higher temperature, resulting in high crystallinity of the samples. Compared with the typical Bi_2Te_3 nanowire sample obtained in TEG, the nanowires that prepared in EG at 180 °C had rough surface and were not uniform (see ESI, Fig. S2a†). The XRD pattern indicated that the crystallinity of the product was poor (see ESI, Fig. S2b†). If the reaction was carried out in H_2O at 100 °C for 20 min, we could not get the phase of Bi_2Te_3 at all (see ESI, Fig. S3). The above results proved undoubtedly that the high-quality Bi_2Te_3 nanowires could not be prepared at a low temperature.

Additionally, we also carried out the template-directed synthesis through the solvothermal route by using a Teflon-lined stainless steel autoclave. Fig. 5 showed the XRD patterns of the samples that were obtained after 12 h solvothermal reaction at 140 °C, 160 °C, 180 °C, and 200 °C, respectively. It is obvious that when the temperature was lower than 180 °C, there was always Te phase residue in the final products (Fig. 5a–c). And when the reaction processed at 200 °C, pure Bi_2Te_3 phase was achieved though, the crystallinity was still not good (Fig. 5d).

Therefore we can conclude that in order to get high-quality Bi_2Te_3 nanowires, heating mantle is better than Teflon-lined stainless steel autoclave basing on the following two reasons: (i) heating mantle has better heat transfer performance than autoclave, which can effectively improve the reaction rate and short the reaction time; (ii) keeping the reaction proceed at reflux by

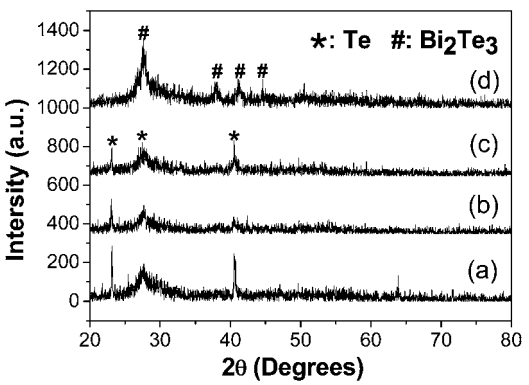

Fig. 5 XRD patterns of the samples obtained after solvothermal reaction for 12 h at (a) 140 °C, (b) 160 °C, (c) 180 °C, and (d) 200 °C respectively.

heating mantle can provide a stable atmospheric pressure environment, while the higher pressure generated in enclosed autoclave at high temperature may destroy the ultrathin wire-like nanostructure (see ESI, Fig. S4†).

Subsequently, the time-dependent experiments were performed in order to understand the growth mechanism of the Bi_2Te_3 nanowires. The samples obtained at different stages of the template-assisted reaction between Te nanowires and $Bi(NO_3)_3$ in TEG were characterized by TEM and XRD. The XRD patterns shown in Fig. 6a–d exhibited the temperature-dependent gradual conversion process from Te templates to Bi_2Te_3 nanowires. When the solution was heated up to 100 °C, the sample phase was transformed from the pure Te (Fig. 6a) to a mixture of Te and Bi (Fig. 6b). After the reaction temperature reached to 160 °C, both Te and Bi phases disappeared and a new phase of Bi_2Te_3 emerged (Fig. 6c). As the reaction processing, the crystallinity of the Bi_2Te_3 became better and better while the reaction temperature reached to 200 °C and maintained for 20 min (Fig. 6d).

TEM images in Fig. 7a–d showed the morphology changes of the products at the different reaction stages. The nanoparticles attached to the Te nanowires shown in Fig. 7a could convey the generation of Bi phase. When the reaction temperature increased to 160 °C, the sample with a tube-like nanostructure could be observed obviously in Fig. 7b and the diameter of the nanotubes was a little larger than the Te nanowires template. Finally, after reaction for 20 min at 200 °C, the tube-like nanostructure disappeared and the uniform Bi_2Te_3 nanowires with smooth surface and high aspect ratio were yielded (Fig. 7c). If the reaction time was prolonged to more than 20 min, the nanowire structure would be broken (Fig. 7d).

On the basis of the above results, it can be speculated that the whole synthetic process of Bi_2Te_3 nanowires includes both Kirkendall effect and Ostwald ripening. In the first step, the Bi^{3+} ions was reduced by hydrazine hydrate to Bi atoms attached to the surface of Te nanowire templates under the action of PVP (Fig. 7a, Scheme 1a and 1b).[35] Then, the composite nanowires were transformed to Bi_2Te_3 nanotubes through the nanoscale Kirkendall effect.[28] The diffusion rate of the Te atoms was larger than that of Bi atoms, which resulted in a net outward flow and

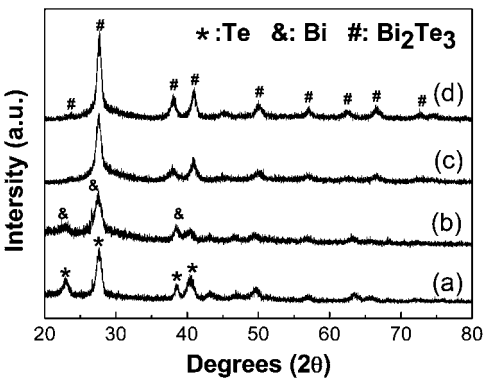

Fig. 6 The XRD patterns of the samples obtained at different stages within the whole reaction: (a) Te nanowire templates and the samples obtained when the solution was heated up to 100 °C (b), 160 °C (c), and reached to 200 °C and maintained for 20 min (d).

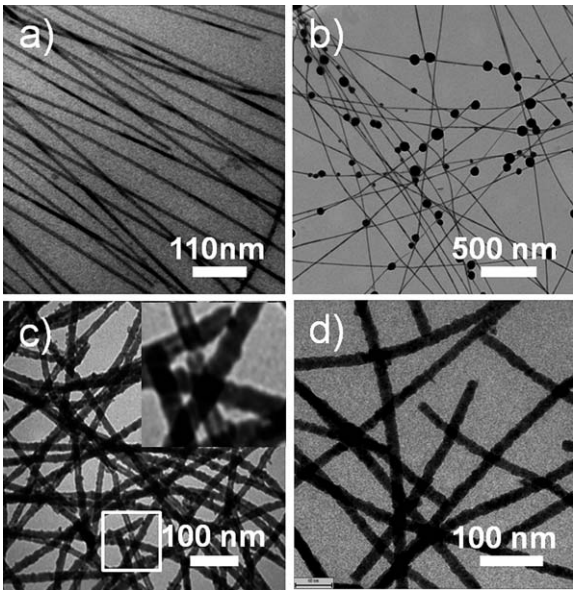

Fig. 7 TEM images of the samples obtained at different stages within the whole reaction process: the samples obtained when the solution was heated up to (a) 100 °C, (b) 160 °C, (c) reached 200 °C and maintained for 20 min, the inset was the magnifying image of the selected area, and (d) maintained at 200 °C for another 20 min.

leads to the formation of hollow tube-like nanostructure (Fig.7b, Scheme 1c). This reaction step can also be proved by the HRTEM images that showed in Fig. 8. Fig. 8a indicated that a bit of Bi_2Te_3 phase began to appear at the edge of Te nanowires when the solution temperature reached 100 °C. Finally, the Bi_2Te_3 nanotubes gradually evolved into uniform Bi_2Te_3 nanowires by the Ostwald ripening process (Fig.7c, Scheme 1d).[37,38] The HRTEM image of the sample obtained after the reaction for 5 min at 200 °C could confirm the transformation from the hollow tube-like Bi_2Te_3 nanostructure to nanowires (Fig. 8b). The whole template reaction under the present conditions could be illustrated as follows:

$$4Bi^{3+} + 3N_2H_4 + 12OH^- \rightarrow 4Bi + 3N_2 + 12H_2O \quad (1)$$

$$2Bi + 3Te \rightarrow Bi_2Te_3 \quad (2)$$

In order to examine whether the obtained uniform Bi_2Te_3 nanowires can enhance the thermoelectric properties effectively, we investigated the electrical and thermal transport properties of

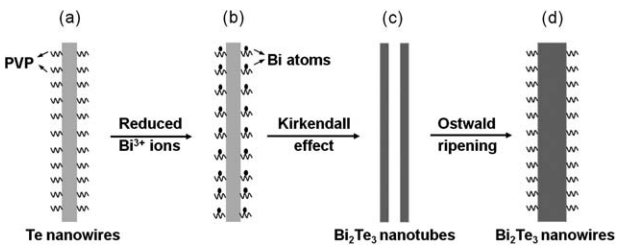

Scheme 1 Schematic illustration of the formation mechanism of the Bi_2Te_3 nanowires *via* a template-assisted solution phase process.

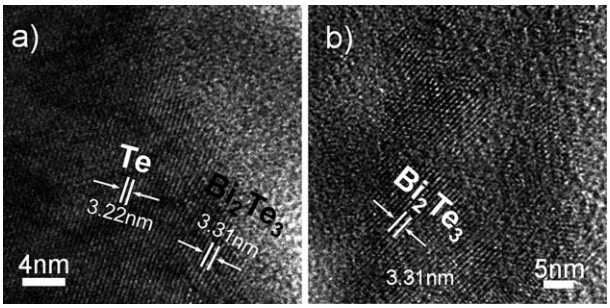

Fig. 8 HRTEM images of the samples obtained (a) when the solution was heated up to 100 °C and (b) maintained at 200 °C for 5 min.

the pellet made up of as-synthesized Bi_2Te_3 nanowires powder. The measured temperature dependence of thermal conductivity, Seebeck coefficient, electrical resistivity and the calculated figure of *ZT* of the bulk material were showed in Fig. 9a–d. It could be seen obviously that the thermal conductivity (κ) was only 0.42 $Wm^{-1}K^{-1}$ at room temperature of 300 K (Fig. 9b), which is strikingly lower than that of other nanostructures of Bi_2Te_3.[3,16] It also proved that one-dimensional nanostructure of thermoelectric materials can indeed decrease the thermal conductivity through enhancing the phonon scattering effect.[4] The Seebeck coefficient (*S*) of the Bi_2Te_3 nanowires pellet had a value of -74 μVK^{-1} at 300 K (Fig. 9a), which illustrated that the sample was a typical *n*-type semiconductor. However, the electrical resistivity (ρ) was only 7.5×10^{-4} Ωm (Fig. 9c), which was lower than that of bulk Bi_2Te_3 materials. The lower electrical resistivity Bi_2Te_3 nanowires were probably resulted from the pressing method where a lower pressure and temperature were applied. Therefore, the density of the obtained nanowires pellet here is still not comparable with the corresponding bulk materials. The SEM image showed in Fig. S5† also indicated that there were still many pores in the pellet, confirming the Bi_2Te_3 nanowires in pellet were just simply compacted into a more dense structure. Another possible factor is the presence of the residual organics in the sample that will also reduce the resistivity. So the figure of the *ZT* in this work was only 0.005 at 300 K (Fig. 9d). The emphasis of the future work will focus on how to convert the nanowires into bulk materials effectively, such as using other pressing methods like spark plasma sintering (SPS) or trying to eliminate the organics on the surface of nanowires.

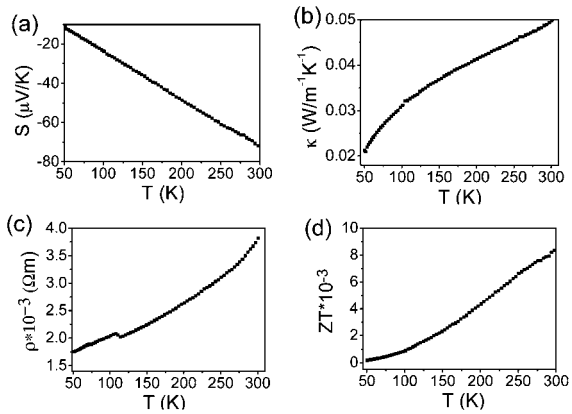

Fig. 9 Transport properties of Bi_2Te_3 nanowires. (a) Seebeck coefficient (mV K^{-1}), (b) Conductivity (W K^{-1}-m), (c) Resistivity (Ohm-m), and (d) Figure of Merit *ZT*.

Conclusions

In summary, uniform Bi_2Te_3 nanowires with high aspect ratio have been synthesized by a template-assisted solution process using ultrathin Te nanowires as template. It has been demonstrated that template-directed synthesis was indeed a convenient and effective way to produce high-quality 1D telluride nanostructures. Based on the temperature dependence of thermal conductivity, Seebeck coefficient and electrical resistivity of the as-pressed pellet, it can be concluded that the thermal conductivity of the 1D Bi_2Te_3 nanowires was indeed decreased, but the electrical resistivity is lower and the figure of *ZT* was not improved. More work is still needed in the future to further improve the thermoelectric performance of the Bi_2Te_3 nanowires.

Acknowledgements

S. H. Y. acknowledges the funding support from the National Basic Research Program of China (2010CB934700), the National Natural Science Foundation of China (Nos. 91022032, 50732006) and International Science & Technology Cooperation Program of China (2010DFA41170).

Notes and references

1 D. M. Rowe, *CRC handbook of thermoelectrics*, CRC Press, Boca Raton, FL, 1995.
2 T. M. Tritt, *Science*, 1999, **283**, 804–805.
3 B. Poudel, Q. Hao, Y. Ma, Y. C. Lan, A. Minnich, B. Yu, X. A. Yan, D. Z. Wang, A. Muto, D. Vashaee, X. Y. Chen, J. M. Liu, M. S. Dresselhaus, G. Chen and Z. F. Ren, *Science*, 2008, **320**, 634–638.
4 M. S. Dresselhaus, G. Dresselhaus, X. Sun, Z. Zhang, S. B. Cronin and T. Koga, *Phys. Solid State*, 1999, **41**, 679–682.
5 Y. M. Lin, X. Z. Sun and M. S. Dresselhaus, *Phys. Rev. B: Condens. Matter Mater. Phys.*, 2000, **62**, 4610–4623.
6 M. S. Dresselhaus, G. Chen, M. Y. Tang, R. G. Yang, H. Lee, D. Z. Wang, Z. F. Ren, J. P. Fleurial and P. Gogna, *Adv. Mater.*, 2007, **19**, 1043–1053.
7 Y. Q. Cao, T. J. Zhu, X. B. Zhao, X. B. Zhang and J. P. Tu, *Appl. Phys. A: Mater. Sci. Process.*, 2008, **92**, 321–324.
8 Y. Q. Cao, X. B. Zhao, T. J. Zhu, X. B. Zhang and J. P. Tu, *Appl. Phys. Lett.*, 2008, **92**, 143106–143108.
9 T. C. Harman, M. P. Walsh, B. E. Laforge and G. W. Turner, *J. Electron. Mater.*, 2005, **34**, L19–L22.
10 M. Zhou, J. F. Li and T. Kita, *J. Am. Chem. Soc.*, 2008, **130**, 4527–4532.
11 R. Venkatasubramanian, E. Siivola, T. Colpitts and B. O'Quinn, *Nature*, 2001, **413**, 597–602.
12 L. D. Hicks and M. S. Dresselhaus, *Phys. Rev. B: Condens. Matter*, 1993, **47**, 16631–16634.
13 T. C. Harman, P. J. Taylor, M. P. Walsh and B. E. La Forge, *Science*, 2002, **297**, 2229–2232.
14 K. F. Hsu, S. Loo, F. Guo, W. Chen, J. S. Dyck, C. Uher, T. Hogan, E. K. Polychroniadis and M. G. Kanatzidis, *Science*, 2004, **303**, 818–821.
15 Y. Jiang and Y. J. Zhu, *J. Cryst. Growth*, 2007, **306**, 351–355.
16 M. Scheele, N. Oeschler, K. Meier, A. Kornowski, C. Klinke and H. Weller, *Adv. Funct. Mater.*, 2009, **19**, 3476–3483.
17 G. Q. Zhang, W. Wang, X. L. Lu and X. G. Li, *Cryst. Growth Des.*, 2009, **9**, 145–150.
18 Q. Yao, Y. J. Zhu, L. D. Chen, Z. L. Sun and X. H. Chen, *J. Alloys Compd.*, 2009, **481**, 91–95.
19 X. B. Zhao, T. Sun, T. J. Zhu and J. P. Tu, *J. Mater. Chem.*, 2005, **15**, 1621–1625.

20 Y. Jiang, Y. J. Zhu and L. D. Chen, *Chem. Lett.*, 2007, **36**, 382–383.
21 M. S. Sander, A. L. Prieto, R. Gronsky, T. Sands and A. M. Stacy, *Adv. Mater.*, 2002, **14**, 665–667.
22 S. A. Sapp, B. B. Lakshmi and C. R. Martin, *Adv. Mater.*, 1999, **11**, 402–404.
23 J. H. Zhou, C. G. Jin, J. H. Seol, X. G. Li and L. Shi, *Appl. Phys. Lett.*, 2005, **87**, 133109–133111.
24 H. Yu, P. C. Gibbons and W. E. Buhro, *J. Mater. Chem.*, 2004, **14**, 595–602.
25 A. L. Prieto, M. S. Sander, M. Martin-Gonzalez, R. Gronsky, T. Sands and A. M. Stacy, *J. Am. Chem. Soc.*, 2001, **123**, 7160–7161.
26 T. Sun, X. B. Zhao, T. J. Zhu and J. P. Tu, *Mater. Lett.*, 2006, **60**, 2534–2537.
27 W. Wang, X. L. Lu, T. Zhang, G. Q. Zhang, W. J. Jiang and X. G. Li, *J. Am. Chem. Soc.*, 2007, **129**, 6702.
28 G. Q. Zhang, Q. X. Yu, Z. Yao and X. G. Li, *Chem. Commun.*, 2009, 2317–2319.
29 Y. Deng, C. W. Nan, G. D. Wei, L. Guo and Y. H. Lin, *Chem. Phys. Lett.*, 2003, **374**, 410–415.
30 A. Purkayastha, F. Lupo, S. Kim, T. Borca-Tasciuc and G. Ramanath, *Adv. Mater.*, 2006, **18**, 496–500.
31 Y. Deng, Y. Xiang and Y. Z. Song, *Cryst. Growth Des.*, 2009, **9**, 3079–3082.
32 H. W. Liang, S. Liu and S. H. Yu, *Adv. Mater.*, 2010, **22**, 3925–3937.
33 G. D. Moon, S. Ko, Y. Min, J. Zeng, Y. N. Xia and U. Jeong, *Nano Today*, 2011, **6**, 186–203.
34 G. D. Moon, S. Ko, Y. Xia and U. Jeong, *ACS Nano*, 2010, **4**, 2307–2319.
35 H. W. Liang, S. Liu, Q. S. Wu and S. H. Yu, *Inorg. Chem.*, 2009, **48**, 4927–4933.
36 H. S. Qian, S. H. Yu, J. Y. Gong, L. B. Luo and L. F. Fei, *Langmuir*, 2006, **22**, 3830–3835.
37 H. C. Zeng, *Curr. Nanosci.*, 2007, **3**, 177–181.
38 J. Zhang, F. Huang and Z. Lin, *Nanoscale*, 2010, **2**, 18–34.

